Turbulence in the solar wind viewed as an anisotropic big-bang

Y. Dong (1), R. Grappin (1), A. Verdini (2)
(1) Laboratoire de Physique des Plasmas LPP
(Ecole Polytechnique, CNRS, UPMC, Univ. Paris-Sud) Palaiseau, France
(2) Università di Firenze, Dipartimento di Fisica e Astronomia, Firenze, Italy
and Royal Observatory of Belgium, SIDC/STCE, Brussels

Abstract

We report here the first results of 3D MHD simulations of turbulence embedded in the solar wind between 0.2 and 1.5 AU. The model (expanding box model) incorporates correctly the basic effects of wind expansion into the MHD equations. Our main results are (i) Expansion **breaks gyrotropy**, that should lead to modify the expression of the injection rate (ii) Expansion induces the **selective decay of the different polarizations** that determines the emergence of coherent structures like microjets (iii) Expansion, together with nonlinear coupling, contribute to drive the dominance of the magnetic spectrum over the velocity spectrum.

Introduction

SW turbulence: ordinary turbulence?

Sketch of turbulent cascade (homogeneous)

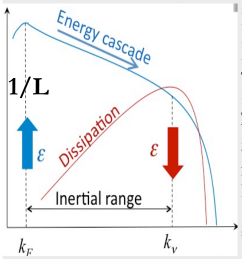

Observations by Coleman (1968) first reported power-law spectra for the magnetic energy on a large frequency range, suggesting a turbulent cascade.
The associated energy flux flowing from large to small scales down to dissipative scales has been found to be indeed ≈ constant (Marino et al. 2011).
A steep $\mathbf{k}_{//}^{-2}$ scaling (instead of $k^{-5/3}$) is found in directions // to the local mean magnetic field (Horbury et al 2008), as expected in strong homogeneous turbulence (critical balance theory).

SW turbulence: odd turbulence?

Several properties however seem to be at odd with usual admitted properties of turbulence
1. Deviations from the standard critical balance theory:
•the *spectral anisotropy* (Forman Wicks Horbury (2011) is best explained by a *contribution of // wavevectors* in contrast to the critical balance prediction
•the galactic cosmic ray modulation also requires a turbulence with a strong contribution of wavevectors // to mean field (Chandran 2000)
•the *flat* ($\propto k^{-3/2}$) scaling of the velocity spectrum (Salem 2000, Podesta 2007, Salem Mangeney Bale Veltri 2009)
•important *deviations from gyrotropy* around the mean field exist (Saur & Bieber 1999, Narita et al 2010)
2. Other specific properties:
•the large magnetic excess found in slow streams (Grappin et al 1991)
•the ordering of polarizations (Belcher & Davis 1971)
•the large cross-helicity in fast streams
•the large-scale k^{-1} scaling atop of the inertial range (figure below)

Double scaling-law

• k^{-1} range has t_{NL} > *transport time* from corona (Carbone Bruno)
⇒ *fossil of coronal turbulence remains k^{-1}* as
• $k^{-5/3}$ range has t_{NL} < transport time (e.g. Tu et al, 1984)
⇒ active nonlinear cascade range

Helios: Magnetic spectra at 0.3, 0.7 and 0.9 AU

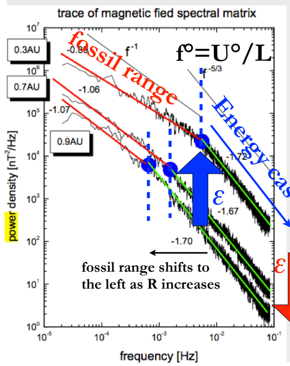

Def.: **fossil range** has *NL time slower than transport time*
⇒ fossil range keeps *k^{-1} imprint of coronal cascade (Verdini et al 2012)*

Hyp.: Inertial range in expanding wind due to quasi-standard NL interactions, BUT injection rate computed on scale L = **largest non-linear scale**

Expanding box model

What expansion does

1. Selective decay of mean quantities
Let us follow a plasma box advected by the solar wind, with uniform speed, expanding radially. During the transport (sketched below), the plasma box gets stretched in directions perpendicular to the radial, so that the different faces of the box increase aither increase as distance R, or as distance squared. Due to this stretching, average (or total) quantities vary:
• mass is conserved, so the mean density decreases as $1/R^2$
• magnetic flux is conserved, so $B_r \propto 1/R^2$, $B_{\theta,\phi} \propto 1/R$
• angular momentum is conserved, so $U_r \propto$ constant, $U_{\theta,\phi} \propto 1/R$
• pressure decreases adiabically at lowest order, so $P \propto \rho^{5/3} \propto R^{-10/3}$

2. Transverse stretching of structures
The expansion of the box is, due to the radial wind, anisotropic, being only in the two directions transverse to radial (see sketch below)
To take it into account, one has to switch to *comobile coordinates that follow the transverse expansion.*

The EBM

This leads finally to the modified MHD equations, written for the basic 8 MHD fields, (density ρ, pressure P, magnetic field **B** and velocity fluctuation **U**), where $\mathbf{U} = \mathbf{V} - U°\hat{e}_r$, **V** being the total velocity, and U° the average wind speed.

$$\begin{aligned}
D_t\rho + \rho\nabla\cdot U &= -2\rho\frac{\epsilon}{a}\\
D_tU + \frac{1}{\rho}(\nabla(P+\frac{B^2}{2}) - B\cdot\nabla B) &= -\alpha U\frac{\epsilon}{a}\\
D_tB - B\cdot\nabla U + B\nabla\cdot U &= -\beta B\frac{\epsilon}{a}\\
D_tP + \frac{5}{3}P\nabla\cdot U &= -\frac{10}{3}P\frac{\epsilon}{a}\\
P &= \rho\, T_p\\
\nabla &= (\partial_x, (1/a)\partial_y, (1/a)\partial_z)\\
a(t) &= R(t)/R = 1+\epsilon t
\end{aligned}$$

Evolution of a plasma box advected by a radial, uniform wind

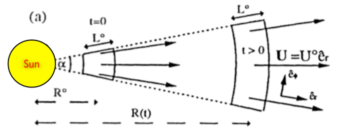

The sketch *above* represents the evolution of a plasma box advected by a uniform radial solar wind with speed U°, starting at distance r=R° with a uniform aspect ratio. Due to the radial wind, the volume is stretched in the two transverse directions and shows an aspect ratio ≈ R/R° as distance has increased from R° to R. This has taken a time t = (R-R°)/U°.
Below a sketch of the EBM model, that uses a pseudo-cartesian coordinate systems (x,y,z) with transversed coordinates comobile with wind expansion.

Evolution of a plasma box in the expanding box model

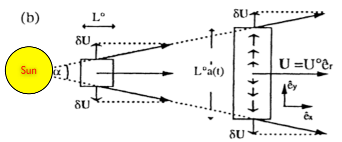

Results (1) Emergence of structures & energy/spectral evolution

List of runs

A: ε=0, B°=0
B: ε=2, B°=0
C: ε=0, B°=2 (radial mean field)
D: ε=2, B°=2 (radial mean field)
E: ε=2, B°=(2,0.2) (oblique mean field)

Initial conditions

Initial distance R°=0.2 AU: isotropic, incompressible (divu=0) K^{-1} spectrum, with equipartition $u^2 \approx B^2$
Zero velocity-magnetic field correlation, Mach ≈ 0.12, $M_{Alfvén}$≈0.5 for runs C, D, E
Expansion parameter **ε = divU/(k°u) = 2** ⇒ *expansion twice as fast as turnover for largest eddies*
(k° = minimum wavenumber = 1; u = rms velocity, divU ≈ 2U°/R° = inverse of transport time, U° = wind velocity)
Note *Daily fluctuations* in the wind have ε≈2 (Grappin Velli Mangeney 1991)
NB. From now on, B is given in Alfvén speed units, i.e., normalized by √<ρ>)
time is given in units of largest scale nonlinear time

Emergence of coherent structures by selective decay of polarizations

Run B (no mean field). Magnetic (left) and Velocity (right) flowlines

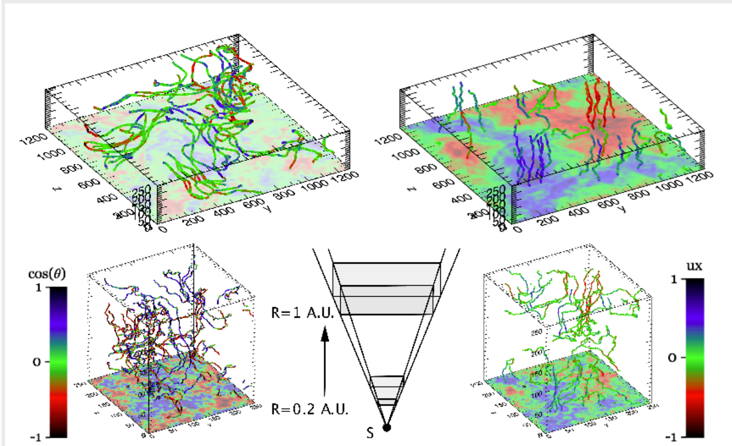

Bottom panels: *initial conditions at 0.2 AU*
Top: *evolution at 1 AU*
Left: *Magnetic field lines*
Right: *Velocity field lines*

Magnetic field lines become ⊥ to the radial

Radial streamlines emerge, resembling microjets.

This results mainly from the *selective decay* of polarizations Bx, Uy, Uz at large scales, due to expansion, i.e., to conservation of magnetic flux and angular momentum :
B_x≈ 1/R
U_y, U_z ≈ 1/R
while other polarizations remain constant

No such selective decay is observed in the test homogeneous simulations.

Energy and spectral evolution

Damping of total (kinetic+magnetic) energy per unit mass

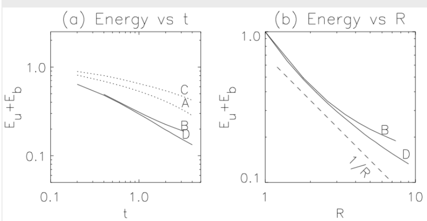

Above
Left: energy decrease with time t
Right: energy decrease with distance R/R°
•No expansion: **mean field slows down energy decrease**
•With expansion: **mean field accelerates energy decrease**

Right:
•formation of a short $K^{-5/3}$ range
•progressive disappearance of the initial k^{-1} scaling

NB K_x = **radial** wavenumber

1D reduced radial total energy spectra compensated by $k^{5/3}$

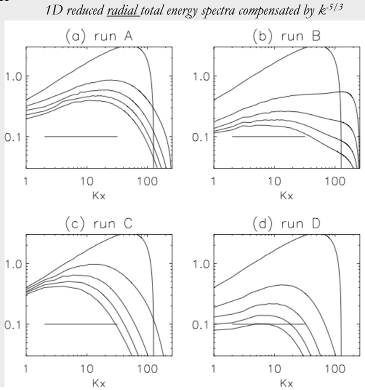

Results (2) Spectral anisotropy

Building spectral anisotropy (1) Nonlinear cascade vs transverse expansion

Homogeneous runs: A & C — *Magnetic energy spectra isocontours at time t=2 in (Kx, K⊥) plane* — *"Expanding" runs: B & D*

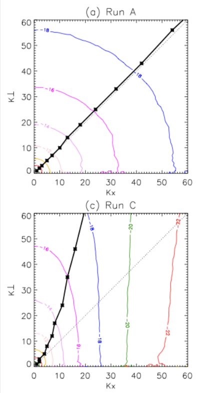

Run A (test case)
no mean field, no expansion
Cascade is isotropic, as shown by black points (thick line) measuring the isocontours aspect ratio at each wavenumber

Run B
no mean field
Dominant cascade is radial as shown by aspect ratio
Interpretation (below) is that kinematic expansion ⊥ to radial fights against nonlinear cascade in the ⊥ directions

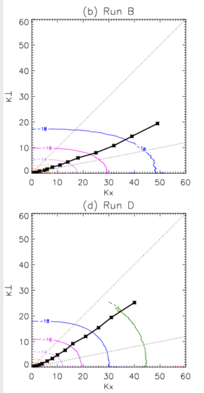

Run C (test case)
with mean field B°=(2,0), no expansion
Dominant cascade is perpendicular to radial, being ⊥ to mean field, as coupling is more resonant in the directions ⊥ to mean field, here the radial

Run D
with mean field B°=(2,0)
Dominant cascade is radial due to fight between
(i) nonlinear-coupling favoring ⊥ directions
(ii) kinematic ⊥ expansion

Building spectral anisotropy (2) generalizing to oblique field

Run D: radial mean field — *Run E: oblique mean field*

Sketch of (homogeneous) cascade ⊥ to mean field

Sketch of (*no mean field*) cascade with kinematic compression ⊥ to radial

True isocontours in the two cases: run D left, run E right.

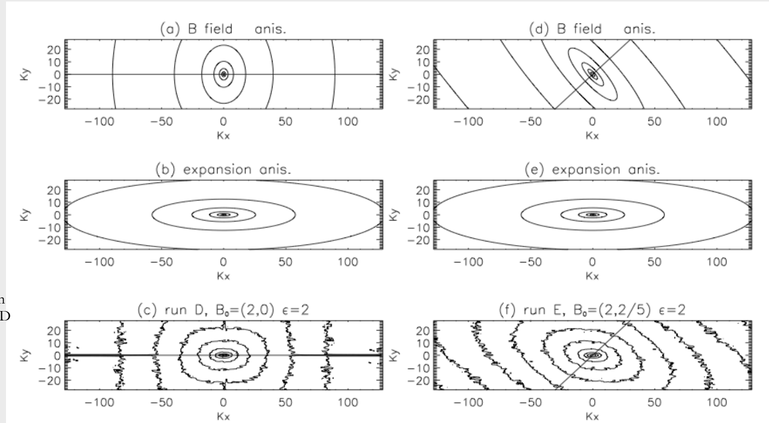

The most realistic **oblique field case** shows scale-dependent anisotropy:
- radial cascade dominates at the largest scales (see bottom panel, right)
- oblique cascade (⊥ to mean field) more and more dominant at smaller scales.

However, the imprint of the kinematic transverse expansion appears even at small scales

Results (3) Anisotropic damping

Magnetic energy modes vs heliocentric distance

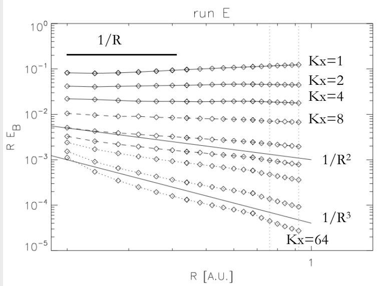

Above: Run E, oblique mean field, decay of magnetic energy at different increasing wavenumbers

Below: isocontours of power-law index α of radial decay rate computed during a limited time interval 1.4<t<1.8 (0.76<R<0.96 AU), for three runs B, D, E.
solid: α =1; dashed: α =2; dotted: α =3
Radial decay is always fastest at all scales than perpendicular decay.
Run E with oblique field shows fight between oblique (mean field) and radial symmetry: gyrotropy is NOT satisfied at all scales.

Radial decay index for total energy vs wave vector

run B: no mean field

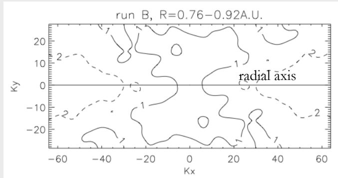

run D: radial mean field

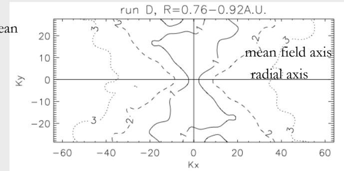

run E: oblique mean field

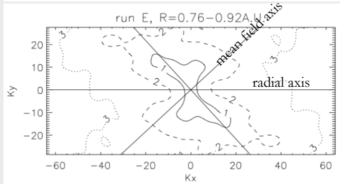

Results (4) Polarization anisotropy

Polarization spectra (Wind data)

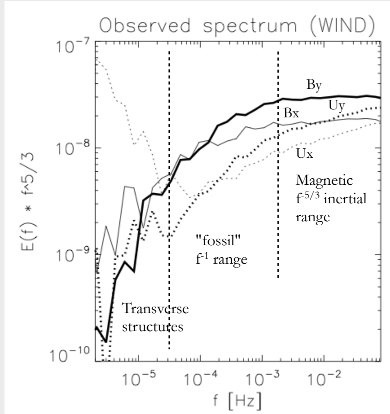

Wind data (high-frequency range) — *Run B: reduced polarization spectra E(Kx)*

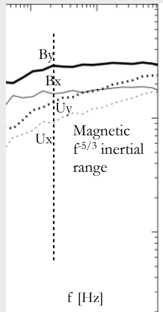

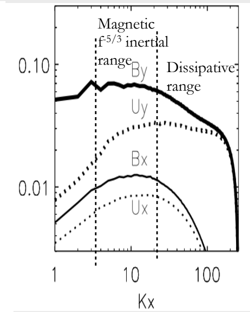

Inertial range dominance of magnetic spectrum over kinetic spectrum can be explained as in Müller & Grappin 2005 by a competition between:
- linear Alfvén effect that forces equipartition (i.e. propagation along local mean field)
- nonlinear local dynamo that transforms kinetic into magnetic energy

The spectral variation of the magnetic excess is explained as follows:
- Alfvén effect wins at small scales
- nonlinear dynamo wins at large scales

Due to conservation of magnetic flux and angular momentum, expansion
- enhances magnetic excess for ⊥ polarizations
- decreases magnetic excess for radial polarizations

Conclusion

We have shown that expansion
- breaks the gyrotropy around the mean field that is usually assumed to be true on the basis of non-expanding phenomenologies of turbulence
- leads to coherent structures akin to observed ones (e.g., microjets)
- leads to magnetic excess as observed, the excess vanishing at the high end of the MHD inertial range

Future work using 3D expanding box model will
- consider separately fast and slow winds
- consider more realistic initial coronal conditions, as
- non-isotropic conditions
- dominance of outward propagating waves when dealing with a mean magnetic field

Bibliography

Bavassano, B., Dobrowolny, M., Fanfoni, G., Mariani, F. & Ness, N. F. *Solar Physics* **78,** 373–384 (1982).
Carbone, V., Malara, F. & Veltri, P. *Journal of Geophysical Research (ISSN 0148-0227)* **100,** 1763–1778 (1995).
Grappin, R. AIP Conf. Proc. **382,** 306–309 (1996).
Grappin, R. & Velli, M. *Journal of Geophysical Research* **101,** 425–444 (1996).
Grappin, R., Velli, M. & Mangeney, A. *Phys. Rev. Lett.* **70,** 2190–2193 (1993).
Matthaeus, W. H., Goldstein, M. L. & Roberts, D. A. *Journal of Geophysical Research (ISSN 0148-0227)* **95,** 20673–20683 (1990).
Müller, W.-C. & Grappin, R. *Phys. Rev. Lett.* **95,** (2005).
Narita, Y., Glassmeier, K.-H., Sahraoui, F. & Goldstein, M. L. *Phys. Rev. Lett.* **104,** 171101 (2010).
Saur, J. & Bieber, J. W. *Journal of Geophysical Research* **104,** 9975 (1999).
Tu, C.-Y., Pu, Z.-Y. & Wei, F.-S. *Journal of Geophysical Research (ISSN 0148-0227)* **89,** 9695 (1984).
Verdini, A., Grappin, R., Pinto, R. & Velli, M. *The Astrophysical Journal Letters* **750,** L33 (2012).